

---

# Leveraging Pre-trained and Transformer-derived Embeddings from EHRs to Characterize Heterogeneity Across Alzheimer’s Disease and Related Dementias

---

Matthew West<sup>1,2</sup>, Colin Magdamo<sup>2</sup>, Lily Cheng<sup>2</sup>, Yingnan He<sup>2</sup>, Sudeshna Das<sup>2</sup>

<sup>1</sup>Department of Biostatistics, Harvard T.H. Chan School of Public Health, Boston, MA

<sup>2</sup>Department of Neurology, Massachusetts General Hospital and Harvard Medical School, Boston, MA

Correspondence: sdas5@mgh.harvard.edu

## ABSTRACT

Alzheimer’s disease is a progressive, debilitating neurodegenerative disease that affects 50 million people globally. Despite this substantial health burden, available treatments for the disease are limited and its fundamental causes remain poorly understood. Previous work has suggested the existence of clinically-meaningful sub-types, which it is suggested may correspond to distinct etiologies, disease courses, and ultimately appropriate treatments. Here, we use unsupervised learning techniques on electronic health records (EHRs) from a cohort of memory disorder patients to characterise heterogeneity in this disease population. Pre-trained embeddings for medical codes as well as transformer-derived Clinical BERT embeddings of free text are used to encode patient EHRs. We identify the existence of sub-populations on the basis of comorbidities and shared textual features, and discuss their clinical significance.

## 1 Introduction

Alzheimer’s disease (AD) is a degenerative neurological condition which affects around 50 million people globally, and is the 6th leading cause of death in the US [1]. Despite its substantial public health burden, AD remains poorly understood and there are relatively few interventions or treatment options available. AD is a type of dementia, a syndrome that emerges following neurodegeneration, and typically affects memory, cognition and behaviour. Alzheimer’s disease and related dementias (ADRD) is an umbrella term that refers to AD and a number of associated common dementias, including frontotemporal dementia (FTD), Lewy body dementia (LBD), and vascular dementia. AD is the most common among the ADRD pathologies, and constitutes around 60-80% of all dementias, being distinguished from other dementias by exerting more significant impact on memory [1].

Pathophysiologically, AD is characterised by the build-up of amyloid- $\beta$  plaques and neurofibrillary tangles constituted by hyperphosphorylated tau proteins. The so-called ‘amyloid hypothesis’ has prevailed as the leading explanation of disease etiology, where it is held that amyloid- $\beta$  toxicity leads to synaptic dysfunction and neurodegeneration [2]. However, while most treatments in development have aimed to target this amyloid hypothesis, existing treatments exhibit borderline efficacy or only show benefit limited to small subpopulations. This motivates an approach to disease characterisation where potential subtypes of disease could be elucidated, thereby informing different disease etiologies, trial designs, and ultimately the development of effective treatments.

Previous approaches to subtyping Alzheimer’s disease have focused on molecular subtyping on the basis of RNA expression, as well as subtyping and staging on the basis of brain imaging and cognitive assessments. Neff *et al.* [3] use RNA-seq signatures from the brain to identify five molecular subtypes of AD in three major classes, characterised by different combinations of multiple dysregulated pathways. These broadly pertain to tau-mediated neurodegeneration, amyloid- $\beta$  neuroinflammation, synaptic signaling, immune activity, mitochondria organization, and myelination.

Using imaging data from patients with FTD and AD, the SuStaIn (Subtype and Stage Inference) algorithm is able to extract disease stage and subtype by training a probabilistic generative model of disease progression on time-series of MRI images [4]. From this, three distinct trajectories of AD were identified, characterised anatomically by the rate

and sequence of atrophy in different brain regions. The SuStaIn algorithm was later applied to a multi-site cohort of positron emission tomography (PET) scans, revealing distinct trajectories of tau deposition in AD [5].

There has also been prior work characterising subtypes of disease based on neuropsychological profiles assessed from cognitive tests. These broadly group patients on the basis of memory, visuospatial and linguistic capabilities, and executive function [6, 7, 8]. Aside from molecular, imaging, and cognitive data, some prior work clustering AD has utilised electronic health records (EHRs) as a modality. EHRs offer easy access to large observational datasets for clinical research, but are subject to their own inherent biases due to not being designed for research purposes. Unsupervised learning on EHR datasets has been leveraged successfully to reveal latent structure in other neurological and neurodevelopmental conditions, such as autism [9, 10], as well as Parkinson’s disease [11].

In the context of Alzheimer’s disease, these EHR-based approaches have been applied with some success, with varying results dependent on methodology and population. Xu *et al.* [12] train an AD risk-prediction model on an EHR-derived cohort, using structured features like diseases and medications to predict EHR-derived AD status. They then cluster representations for AD patients derived from predictive features in the risk-prediction task, identifying subtypes by prevalence of comorbidities and medications. These subtypes broadly correspond to patients with cardiovascular disease, those with mental illness, those with older age of onset, and finally those taking medications for dementia and with sensory problems.

Alexander *et al.* [13] use a large EHR system to characterise the clinical heterogeneity of AD, using diagnoses, symptoms, and demographic data from a literature-informed feature set to characterize patients. They provide a comparative analysis of four different clustering methods and assess the stability and reproducibility of the phenotypic clusters that are identified. They reliably identify a subpopulation of early-onset AD patients characterised by a faster rate of progression and being predominantly female. The approach in Landi *et al.* [14] utilises unsupervised deep learning to derive representations of EHRs from an entire hospital system, without restriction to any one disease cohort. To derive these representations, they explicitly encode each EHR in a temporal sequence, constituted by diagnoses, medications, labs, and procedures along with pre-trained word embeddings to characterise medical concepts extracted from notes. These representations are passed through a convolutional autoencoder, and latent representations are retained to cluster patients. Following training, they cluster on patient representations to try and identify separation between 8 disease groups, before attempting to characterize heterogeneity within disease group. One of these disease groups is AD, where they identify three distinct clusters: patients with early-onset disease, patients with later-onset disease and mild neuropsychiatric and cerebrovascular comorbidities, and finally patients with typical onset and mild-to-moderate dementia symptoms.

More recently, He *et al.* [15] performed a spectral clustering on a cohort of patients EHRs, using features derived in a 3-year window prior to AD onset. They specifically encode diagnoses prior to AD onset in discrete 6-month intervals, and identify four clusters that differ significantly in terms of demographics, mortality, and prescription medications. Tang *et al.* [16] perform a deep clinical phenotyping on the basis of comorbidities in patient EHRs from two independent cohorts, and identify a number of clusters that appear to exhibit dependence on sex. For example, after sex stratification there is an enrichment for vascular and musculoskeletal disorders in females with AD vs female controls, and enrichment for behavioural/neurological disorders in males with AD vs male controls. They also characterise network interactions between comorbidities in AD patients, which compared to controls exhibit greater numbers of edges and higher rates of comorbid conditions.

Building on these studies, the methodology contained in this work offers the following contributions:

- We make use of pre-trained embeddings from a medical context to encode ICD codes prior to clustering.
- In contrast to prior work, we make direct use of clinical free-text without prior rule-based extraction of medical concepts.
- We demonstrate the use of transformers adapted to a clinical domain to encode representations of clinical text, and that these representations are able to characterise heterogeneity in AD following clustering.

In this work, we both utilise both pre-trained embeddings for ICD code diagnostic data and transformer-derived embeddings to characterise clinical notes, clustering patient representations for each of these modalities independently. Transformers are a recent development in deep learning that have exhibited state-of-the-art performance in language modelling tasks, and are broadly characterised by their reliance on the concept of attention [17]. Attention, so-called because it mimics cognitive attention, allows contextual information to be shared between word representations without explicitly encoding word sequence, by providing attention weights to bias important parts of prior representations in the network’s forward pass. The transformer used in this work is a version of the BERT architecture fine-tuned on a biomedical corpus [18]. BERT allows for improved contextual representations over the original transformer architecture, with its base architecture having 12 attention heads in each of its 12 layers, allowing for more detailed contextual word

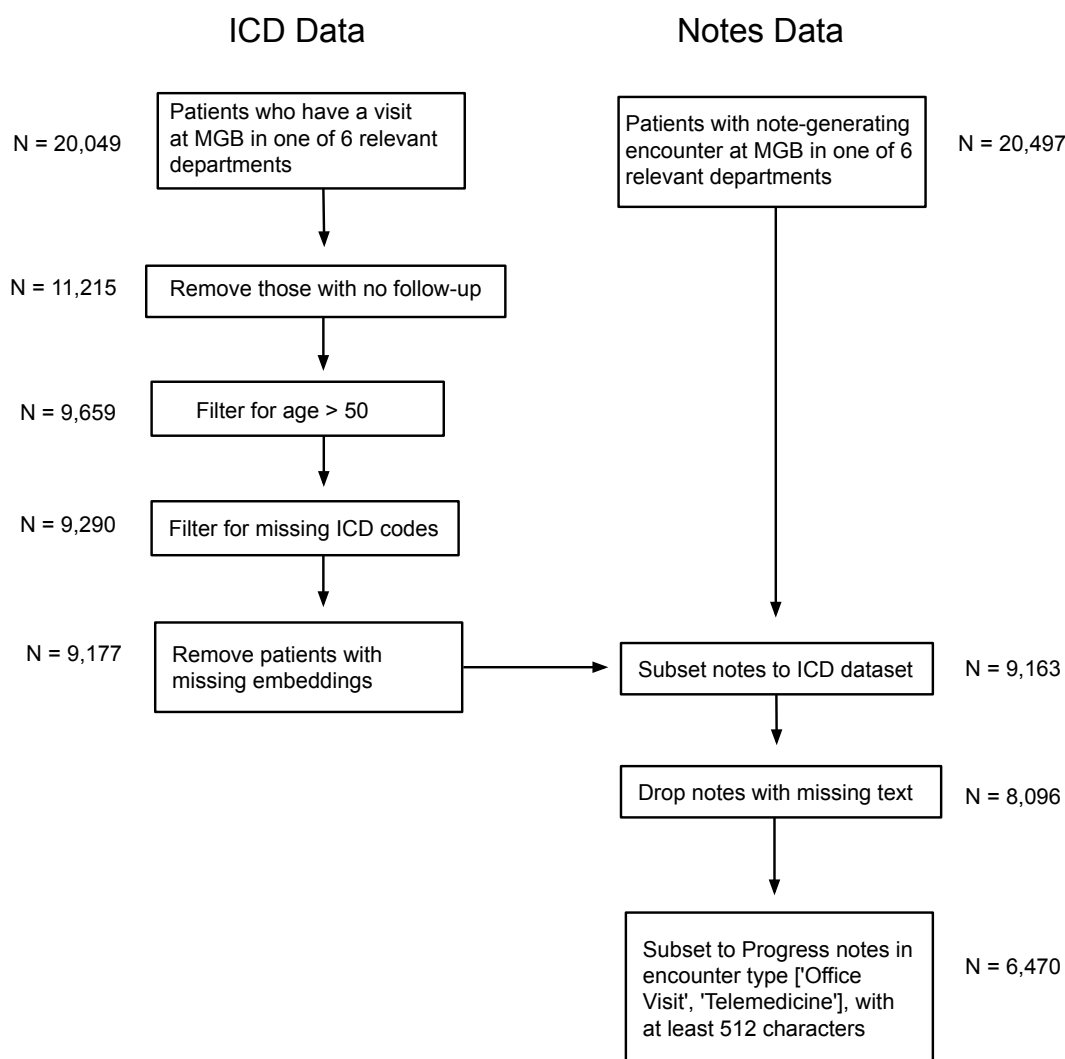


Figure 1: **Cohort selection process.** A flowchart showing the cohort selection process for the our patient cohort.

embeddings. This architecture provides an encoder which can be fine-tuned on downstream applications and domains, as done in BioBERT, which fine-tunes the BERT-base architecture on PubMed abstracts and PMC full-text articles [19]. Specifically, we use Clinical BERT, a publicly-released model which further fine-tunes BioBERT on notes from the critical care database MIMIC [20, 21].

## 2 Methods

### 2.1 Cohort Selection Process

Patients were queried from the Mass General Brigham (MGB) Research Patient Data Registry (RPDR) query tool, where  $N = 20,497$  candidate patients having at least one note-generating encounter in one of 6 relevant departments having memory specialists were identified. Patients were drawn mainly from the Memory Disorders Unit at Massachusetts General Hospital (MGH), as well as patients seen by memory specialists at Brigham and Women’s Hospital (BWH). Two datasets were extracted in parallel for the patient cohort identified, one of structured diagnostic ICD code data, as well as one of unstructured clinical notes written by a neurologist. Access to this data for research purposes was approved by the Mass General Brigham Institutional Review Board (IRB).

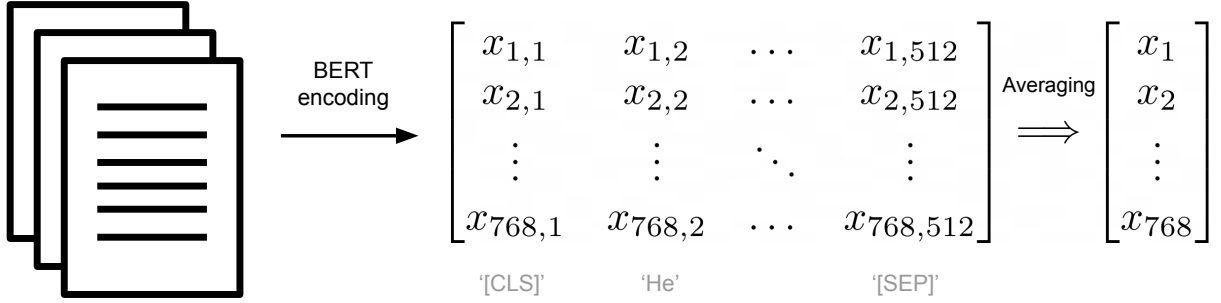


Figure 2: **Notes preprocessing pipeline visualization.** A schematic diagram showing the note processing pipeline for a 512-token input sequence to Clinical BERT.

$N = 20,049$  patients were identified from memory disorder department visits on the basis of ICD codes alone. Subsetting to those with at least one follow-up encounter, having an age at first encounter greater than 50 years, and filtering for missing ICD9 codes yielded  $N = 9,290$ . After converting patient records to vector representations using pre-trained embeddings, patients with missing embeddings were dropped to yield an ICD dataset of  $N = 9,177$  patients. After dropping patients without notes from a neurologist encounter, and selecting for only substantial notes ( $\geq 512$  characters) documenting office visits or telemedicine encounters, the final cohort was constituted by  $N = 6,470$  patients. This cohort selection process is shown in more detail in Fig. 1.

For characterising our ADRD phenotype in the cohort and in our resultant clusters, the presence of at least one relevant ICD9 code for each disease group was used. For AD this was 331.0, and for FTD this was 331.1 (FTD), 331.19 (other FTD) and Pick’s disease (331.11). For LBD, 331.82 was used, and vascular dementia was defined by having any of 290.40 (uncomplicated), 290.41 (with delirium), 290.42 (with delusions), or 290.43 (with depressed mood). Finally, MCI was defined by the presence of 331.83, and memory loss by 780.93.

## 2.2 Embedding Methodology

### 2.2.1 ICD Codes

Prior to clustering, it was necessary to derive a patient-level representation that encodes information relevant to phenotype in a single vector. While some prior work has relied on one-hot encoding of clinical data to represent patient phenotype, we leverage existing pre-trained embeddings that capture relevant biomedical semantics in their latent representations of clinical concepts. In particular, we use a set of 300-dimensional embeddings for ICD9 codes, derived from prior work by Choi *et al.* [22]. For a one-hot encoded representation of  $m$  ICD9 codes across our cohort,  $\mathbf{P} \in \mathbb{R}^{6470 \times m}$ , and an embedding matrix,  $\mathbf{E} \in \mathbb{R}^{m \times 300}$ , our design matrix for clustering,  $\mathbf{X} \in \mathbb{R}^{6470 \times 300}$ , is given by the following matrix multiplication:

$$\mathbf{X} = \mathbf{P} \cdot \mathbf{E}.$$

This matrix multiplication sums the ICD embeddings across a patient record, and the resultant embedding is directly affected by the number of times each code appears in a patient’s history. Another representation for the ICD9 codes was investigated, taking the row-wise mean of embeddings instead of their sum. This amounts to normalising  $X$  by dividing by the row-wise sum of  $\mathbf{P}$ . While these were compared, a more salient and interpretable clustering was observed for the sum of the embeddings for the ICD dataset. A comparison of silhouette scores and inertia also used in determining methodology and number of clusters can be seen in Supplementary Figure 1.

### 2.2.2 Patient Notes

Patient notes were encoded using Clinical BERT prior to clustering. In order to derive patient-level representations from notes, a number of preprocessing steps were undertaken. First, unwanted delimiter characters were stripped from patient notes, and notes were chunked into contiguous sections of 1024 characters. This resulted in a distribution of token numbers of  $\sim 200$ -300 per note following BERT’s WordPiece encoding of input sequences. After passing through the transformer encoding, we took the final layer representation averaged over the 12 attention heads, such that each note was represented by a matrix of dimension  $(768, n)$ , corresponding to each of the  $n$  input tokens having a 768-dimensional contextual vector representing it. Following this encoding, the representation was averaged over the

token dimension, so as to arrive at a single 768-dimensional vector for the whole note. This was explored using both simple averaging over the token dimension, as well as attention-weighted averaging based on row-wise entropy of the final layer attention matrix, and attention-weighted averaging was used in patient representations due to the resultant lower inertia and increased silhouette score on average, and figures demonstrating this can be found in Supplementary Figure 2. A schematic depicting the note representation pipeline can be seen in Fig. 2.

### 2.2.3 Attention-weighted averaging

For a given input sequence of length  $n$ , the final layer representation in a transformer model has an associated self-attention matrix,  $\mathbf{A} \in \mathbb{R}^{n \times n}$ . For BERT-based models,  $n \leq 512$  due to the constraint on the length of the input sequence. In order to provide weights for averaging the embedding,  $\mathbf{E} \in \mathbb{R}^{768 \times n}$ , over the token dimension, we compute the row-wise differential entropy of the attention matrix, given in equation 1. Differential entropy is the continuous analogue of Shannon entropy, which is usually only defined for discrete random variables [23]. In particular, the method described in Ebrahimi *et al.* [24] is used to approximate the differential entropy, implemented in the Python library SciPy [25], as the closed-form expression for the attention distribution for a given row  $f(x)$  is not known analytically from the values of attention sampled. The differential entropy for a row  $i$  is given by

$$h_i = h(A_i) = - \int_{\mathcal{A}_i} f(x) \log(f(x)) dx, \quad (1)$$

and the corresponding vector  $\mathbf{h} \in \mathbb{R}^{n \times 1}$  corresponds to the entropy across every row. From the row-wise entropy, this vector is softmaxed to get the corresponding weights,  $\mathbf{w} \in \mathbb{R}^{n \times 1}$ :

$$w_i = \sigma(\mathbf{h})_i = \frac{e^{h_i}}{\sum_{j=1}^n e^{h_j}}. \quad (2)$$

The resultant note embedding,  $\mathbf{N}$ , is then given by the matrix multiplication

$$\mathbf{N} = \mathbf{E} \cdot \mathbf{w}, \quad (3)$$

and the final patient-level representation is the simple average over all note fragments for a given patient, over all of their encounters. A visualization of attention matrices with varying row-wise entropy and thus varying weighting is given in Supplementary Figures 3 and 4.

## 2.3 Hierarchical Clustering

Following the encoding of both ICD9 codes for the ICD data and clinical text for the notes data, a clustering analysis was performed for each representation. We employed hierarchical agglomerative clustering using Ward’s linkage criterion, implemented in the Python package Scikit-learn [26]. Elbow plots and silhouette scores were used to compare clustering methods and to select the number of clusters for each of the two datasets. Following clustering, resultant clusters were characterised by testing for enrichment of ICD9 codes within each cluster. This enrichment analysis was performed for both the ICD representation and the patient notes representation, even though the codes themselves were not used in clustering the notes representation. Within each cluster, a 2x2 contingency table was generated for each ICD9 diagnosis code, comparing counts of patients with that code within-cluster to counts of patients with that same code in other clusters. The relative prevalence of each code as well as a fold-change between groups was characterised, and a  $\chi^2$  test for enrichment was performed. A Bonferroni correction was applied to the resultant  $p$ -values to correct for multiple comparisons, and ICD codes with positive fold-change were ranked by corrected  $p$ -value to characterise the most significant enrichments. All  $p$ -values in this investigation were two-sided, with a post-corrected  $\alpha$  of 0.05 to determine significance. For clusters derived in the notes clustering, enrichment of words within notes was also characterised by TF-IDF (term frequency–inverse document frequency). In this context, the sum total of all notes within a cluster is considered a document, and the set of stop words utilized was adapted from scikit-learn’s English stop word list to include nonspecific medical terminology.

## 3 Results

Table 1 shows the distribution of characteristics across our selected patient cohort. For this cohort, both ICD-based and notes-based representations from patient EHRs were derived and clustered independently. One thing to note is

the prevalence of AD, as determined by having the relevant ICD code, is relatively low overall. While a significant number of patients lack an ICD diagnosis code for AD, this does not necessarily mean the prevalence of AD is low. Diagnosis is only probable until postmortem examination of brain tissue, and neurologists are typically reluctant to diagnose the condition until patients are further along in the disease course. Therefore, the substantial majority of patients seen in this cohort are likely to have AD or go on to be diagnosed with it at some point. A subset of patients are affected with other dementias, including frontotemporal dementia, Lewy body dementia, and vascular dementia. While the prevalence of vascular dementia is the highest among these, there is some overlap in diagnoses and many of these patients have an AD ICD code alongside their other dementia diagnosis.

### 3.1 ICD Clustering

Three clusters were identified in the ICD representation of patient EHRs. Fig. 3a shows a UMAP [27] projection of the ICD code embeddings, colored by cluster. Fig. 3b shows the same projection but colored by the presence of an AD code, where it can be seen that the main axis of variation in clustering is approximately orthogonal to the axis of variation in AD code presence. This indicates that the phenotypic distinction captured in clustering is not entirely confounded by the presence of the AD code alone, and that clustering is therefore driven by other phenotypic features.

The first cluster ( $N = 508$ ) was characterised by ICD codes for chronic pain and type 2 diabetes (T2D). There was a 3-6 fold increase in prevalence of pain-related codes like foot pain and fibromyalgia compared to patients in other clusters, and approximately 20% of patients within this cluster had T2D codes, compared with a background prevalence of 3% in the other clusters. This cluster was marginally more female and significantly more non-White than the other clusters. The prevalence of AD within this cluster was also lower, though with substantially higher prevalence of mild cognitive impairment or memory loss compared to the cohort average. This may indicate a group of patients earlier on in their timeline of disease progression and diagnosis, though with a larger burden of primary care as indicated by having an increased number of unique ICD codes compared to the cohort average. A higher proportion of patients were genotyped in this cluster but with a lower APOE dosage on average compared to other clusters.

A second cluster ( $N = 4,350$ ) was defined by lack of significant enrichment for the codes as found in the other clusters, and a marginally higher prevalence of neurodegenerative/focal neurological conditions, without being statistically significant, with the exception of frontotemporal dementia and Alzheimer’s disease. This group of patients had lower numbers of unique codes, indicating less of a substantial interaction with the health system outside of their neurology visits. This group also had a significantly lower prevalence of Hispanic patients.

The third and final cluster ( $N = 1,612$ ) was characterised by codes related to cardiovascular and general diseases of aging, as well as some overlap with the pain cohort. Patients within this cluster also had a more general interaction with the healthcare system overall, with enriched codes for routine general examinations and immunization. This may indicate a subset of patients that interacted with the MGB health system substantially for general primary care outside of the neurology department, which is consistent with the increased number of unique ICD codes compared to the cohort average. Patients in this cluster were significantly older at their first and last encounters, and had higher prevalence of

Variable	Value (N = 6,470)
Age at first encounter	72.6 ± 9.8
Age at last encounter	75.2 ± 9.7
Female	3,316 (51.3%)
Race (non-White)	861 (13.3%)
Ethnicity (Hispanic)	275 (4.3%)
With AD code	2,970 (45.9%)
With FTD code	463 (7.2%)
With LBD code	359 (5.5%)
With Vascular dementia code	649 (10.0%)
With MCI/Memory loss code	3,922 (60.6%)
Number of unique codes	36.1 ± 32.5
Number of patients genotyped	487 (7.5%)
APOE dosage	0.55 ± 0.65

Table 1: Patient cohort characteristics. Key: AD = Alzheimer’s disease, FTD = Frontotemporal dementia, LBD = Lewy body dementias, MCI = Mild cognitive impairment.

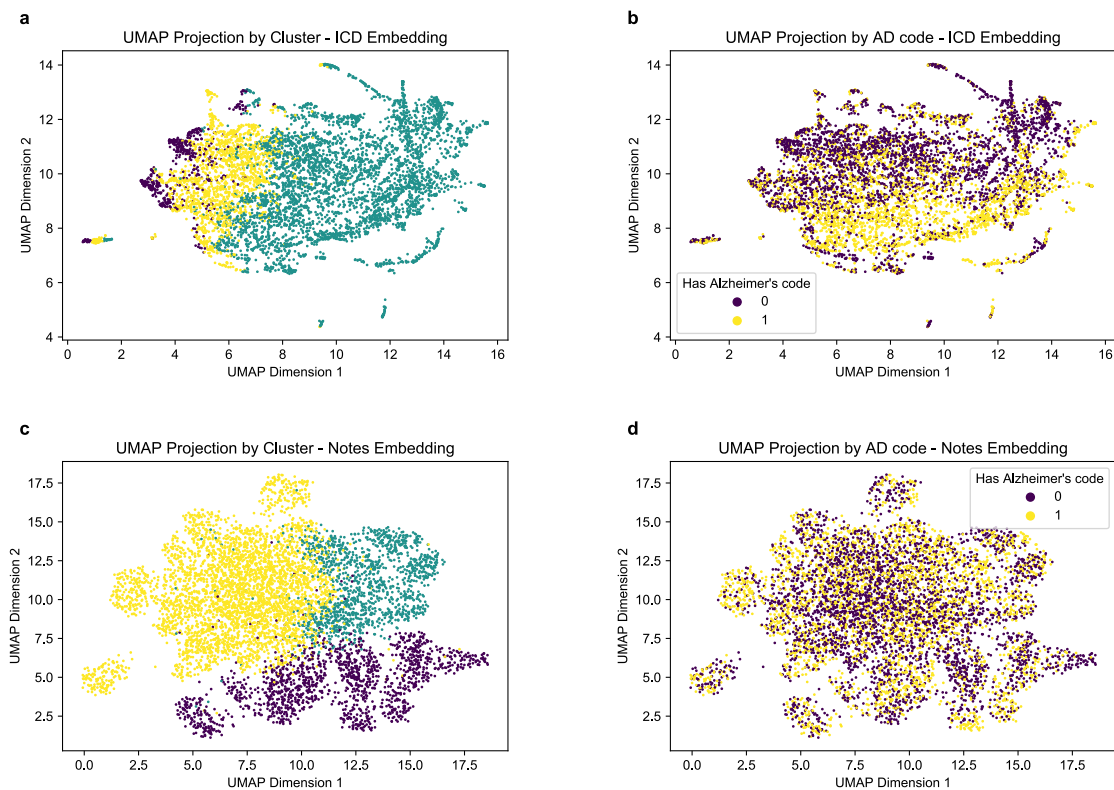


Figure 3: **UMAP projections of patient cohort across both representations.** UMAP projections of the ICD representation coloured by cluster membership (a) and patients having Alzheimer’s ICD9 code (b), as well as the corresponding projection for the patient notes representation (c, d).

vascular dementia and MCI/memory loss compared to the cohort average. Fig. 4 shows representative ICD codes for each of the three clusters, colored by their relative enrichment (row-wise  $Z$ -scores). Table. 2 provides a description of cluster characteristics for the ICD clustering, and tables depicting more detail on the specific ICD codes enriched within each cluster can be found in Supplementary Tables 1-6.

### 3.2 Note Cohort Clusters

Three clusters were also identified in the patient notes clustering. As in the ICD clustering, Fig. 3c shows a UMAP projection of the note embeddings, colored by cluster, and Fig. 3d shows the same projection but colored by the presence of an AD code. Here we again see a clear boundary between clusters in the 2D projection, which appears relatively independent to the prevalence of AD as measured by ICD code. This indicates that the phenotypic distinction captured in clustering is not entirely confounded by the presence of the AD code alone, and that clustering is therefore driven by other phenotypic features.

The first cluster ( $N = 1,469$ ) was characterised by the enrichment for codes related to hydrocephalus, together with codes for Lewy body disease (both Lewy body dementias and Parkinson’s disease). This indicates a patient cluster that overlaps phenotypically in terms of movement disorders and gait. It should be noted that while statistically significant with an approximate 5-fold enrichment, the prevalence of hydrocephalus and (as well as Parkinson’s disease) within this cluster was still relatively low, at around 12%.

The second cluster ( $N = 1,297$ ) identified in the notes clustering was characterised by significantly enriched codes for senile dementia and hypertension, and broadly overlapped in terms of other over-represented codes with the cardiovascular/aging cluster from the ICD clustering. While not significant after correction for multiple comparisons, many other codes for cardiovascular and dermatological conditions exhibit increased prevalence, highlighting that this cluster was also distinguished by a substantial volume of interaction with the MGB system for primary care in addition

Variable	Chronic Pain/T2D (N = 508)	Other Neuro (N = 4,350)	Cardio/Aging (N = 1,612)	p-value
Age at first encounter	72.4 ± 9.7	71.9 ± 9.9	74.7 ± 9.3	< <b>0.001</b> <sup>a</sup>
Age at last encounter	75.0 ± 9.6	74.4 ± 9.8	77.3 ± 9.2	< <b>0.001</b> <sup>a</sup>
Female	295 (58.1%)	2,236 (51.4%)	785 (48.7%)	0.12 <sup>b</sup>
Race (non-White)	92 (18.1%)	544 (12.5%)	241 (15.0%)	<b>0.003</b> <sup>b</sup>
Ethnicity (Hispanic)	31 (6.1%)	149 (3.4%)	95 (5.9%)	< <b>0.001</b> <sup>b</sup>
With AD code	122 (24.0%)	2,177 (50.0%)	671 (41.6%)	< <b>0.001</b> <sup>b</sup>
With FTD code	17 (3.3%)	372 (8.6%)	74 (4.6%)	< <b>0.001</b> <sup>b</sup>
With LBD code	24 (4.7%)	243 (5.6%)	92 (5.7%)	0.714 <sup>b</sup>
With Vascular dementia code	64 (12.6%)	370 (8.5%)	215 (13.3%)	< <b>0.001</b> <sup>b</sup>
With MCI/Memory loss code	395 (77.8%)	2,303 (52.9%)	1,224 (75.9%)	< <b>0.001</b> <sup>b</sup>
Number of unique codes	98.5 ± 36.3	19.9 ± 15.7	64.0 ± 21.5	< <b>0.001</b> <sup>a</sup>
Number of patients genotyped	86 (16.9%)	228 (5.2%)	173 (10.7%)	< <b>0.001</b> <sup>b</sup>
APOE dosage	0.40 ± 0.54	0.60 ± 0.69	0.57 ± 0.65	<b>0.0045</b> <sup>a</sup>

Table 2: ICD clustering characteristics. Key: T2D = Type 2 diabetes, KD = Kidney disease, AD = Alzheimer’s disease, FTD = Frontotemporal dementia, LBD = Lewy body dementias, MCI = Mild cognitive impairment. Statistical tests: <sup>a</sup> one-way ANOVA (*F*-test), <sup>b</sup>  $\chi^2$  test of independence.

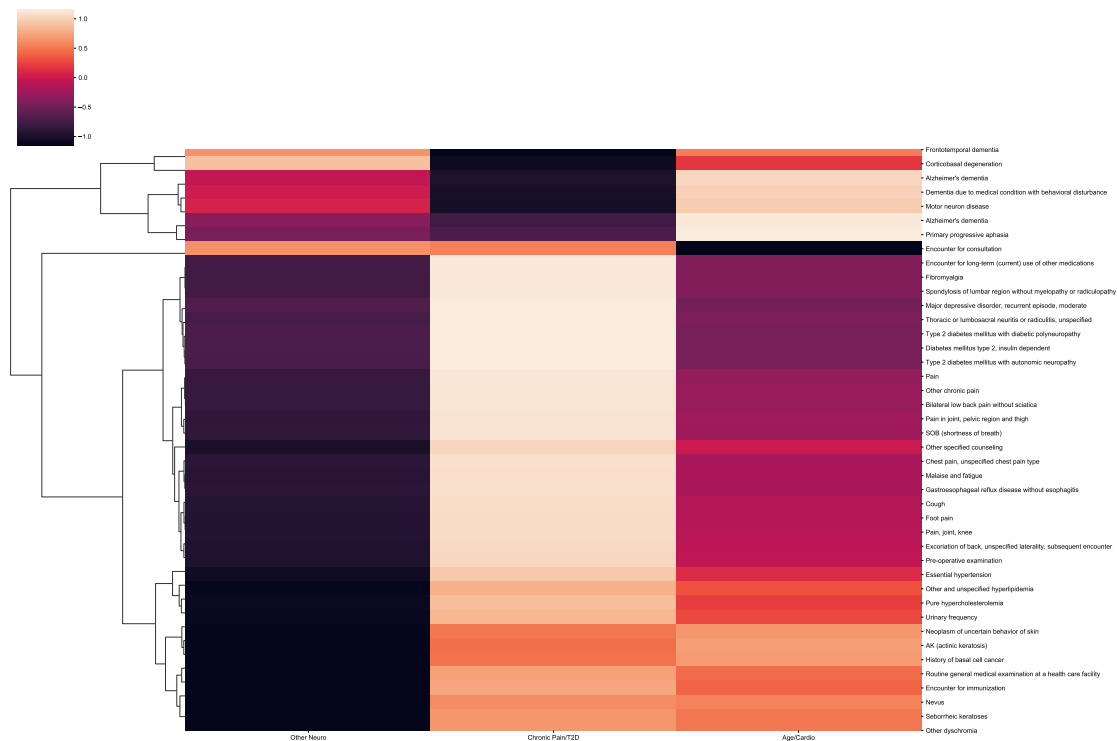


Figure 4: **ICD clustering heatmap.** A heatmap showing ICD9 code enrichment for clusters found in the ICD clustering. The colour of each code-cluster pair is determined by the normalized Z-score for that code.

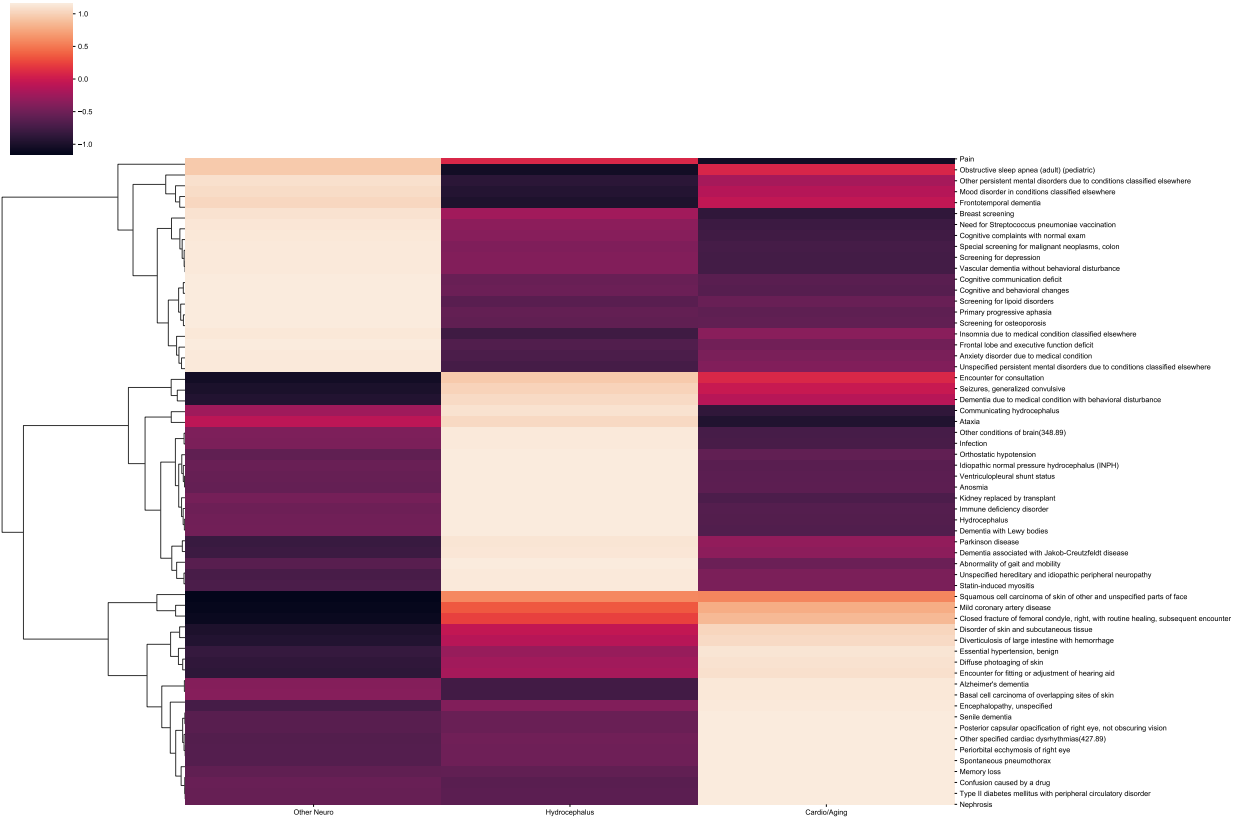


Figure 5: **Notes clustering heatmap.** A heatmap showing ICD9 code enrichment for clusters found in the patient notes clustering. The colour of each code-cluster pair is determined by the normalized Z-score for that code.

to being seen by memory specialists. AD prevalence is higher in this cluster, together with a slightly increased average age at first and last encounter compared to the cohort average.

The third and final cluster ( $N = 3,704$ ) was characterised by a marginally higher prevalence of other neurodegenerative/focal neurological conditions, as also captured in clustering using the ICD representation. This cluster was also significantly enriched for neuropsychiatric conditions, including, mood disorders, anxiety disorder due to a medical condition, and screening for depression. Frontotemporal dementia was again significant, as well as other focal neurological conditions such as vascular dementia and primary progressive aphasia. Also of note for this cluster was the increased prevalence of non-White and Hispanic patients, as well as female patients. Representative codes for these three clusters are visualized in Fig. 5, with this heatmap demonstrating a more disjoint separation in enriched codes than for the ICD clustering, and cluster characteristics for the notes clusters are shown in Table. 3.

In addition to the enrichment for ICD codes, the notes-based clustering was characterised by over-representation for individual words as measured by the TF-IDF statistic, as shown in Table. 4. Despite some overlap between clusters, important words identified in each cluster by TF-IDF were generally concordant with their characterisation from the ICD code enrichment. Within the hydrocephalus/LBD cluster, important words included ‘pain’ and ‘tremor’, which are both specific features of that phenotype. The cardiovascular/aging cluster identified words like ‘scan’, ‘memantine’, and ‘donepezil’, which indicates diagnostic scanning as well as administration of common dementia medications. For the ‘other neuro’ cluster, ‘language’, ‘speech’, and ‘word’ are important, with speech-related symptoms being prevalent in many neurodegenerative conditions, as well as ‘anxiety’ and ‘behavioral’ corresponding to the neuropsychiatric conditions identified as prevalent in this cluster.

## 4 Discussion

The aim of this study was to characterise heterogeneity in Alzheimer’s disease and related dementias, by applying existing representation learning techniques to patient EHRs. To that end, we have leveraged pre-trained embeddings for

Variable	Hydrocephalus/LBD (N = 1,469)	Cardio/Aging (N = 1,297)	Other Neuro (N = 3,704)	p-value
Age at first encounter	73.9 ± 9.5	74.7 ± 9.4	71.4 ± 9.9	< <b>0.001</b> <sup>a</sup>
Age at last encounter	76.8 ± 9.1	77.5 ± 9.2	73.7 ± 9.9	< <b>0.001</b> <sup>a</sup>
Female	696 (47.4%)	611 (47.1%)	2009 (54.2%)	<b>0.007</b> <sup>b</sup>
Race (non-White)	147 (10.0%)	169 (13.0%)	561 (15.1%)	< <b>0.001</b> <sup>b</sup>
Ethnicity (Hispanic)	29 (2.0%)	48 (3.7%)	198 (5.3%)	< <b>0.001</b> <sup>b</sup>
With AD code	638 (43.4%)	662 (51.0%)	1,670 (45.1%)	<b>0.036</b> <sup>b</sup>
With FTD code	57 (3.9%)	66 (5.1%)	340 (9.2%)	< <b>0.001</b> <sup>b</sup>
With LBD code	155 (9.9%)	43 (3.3%)	161 (4.3%)	< <b>0.001</b> <sup>b</sup>
With Vascular dementia code	133 (9.1%)	75 (5.8%)	441 (11.9%)	< <b>0.001</b> <sup>b</sup>
With MCI/Memory loss code	860 (58.5%)	794 (61.2%)	2,268 (61.2%)	0.654 <sup>b</sup>
Number of unique encounters	4.9 ± 3.8	4.5 ± 3.9	4.9 ± 6.2	0.090 <sup>a</sup>
Number of patients genotyped	119 (8.1%)	114 (8.8%)	254 (6.9%)	0.075 <sup>b</sup>
APOE dosage	0.55 ± 0.65	0.51 ± 0.60	0.57 ± 0.68	0.664 <sup>a</sup>

Table 3: Patient notes clustering characteristics. Key: AD = Alzheimer’s disease, FTD = Frontotemporal dementia, LBD = Lewy body dementias, MCI = Mild cognitive impairment. Statistical tests: <sup>a</sup> one-way ANOVA ( $F$ -test), <sup>b</sup>  $\chi^2$  test of independence.

Hydrocephalus/LBD	Cardio/Aging	Other Neuro
bp	recall	social
vitamin	scan	anxiety
tremor	decline	speech
oral	donepezil	language
nightly	memantine	behavioral
route	behavioral	bilaterally
active	work	pain
outpatient	driving	word
pain	social	recall
mood	language	attention

Table 4: TF-IDF for enriched words within each cluster.

ICD codes and a state-of-the-art transformer architecture to encode patient notes, which have not been applied before in the context of unsupervised learning on EHRs for AD. In doing so, we have identified a number of well-defined phenotypes based on prevalent ICD codes within the resultant clusters.

These clusters arose after deriving two independent representations on the basis of data modality, one from structured patient ICD codes, and one from unstructured neurology notes. We identified three clusters in both the ICD representation and the patient notes representation, with a substantial degree of overlap in identified clusters between the two modalities. In the ICD clustering, a cluster was identified that was clearly characterised by the presence of codes related to chronic pain and type 2 diabetes. This cluster maps to a T2D cluster identified in Xu *et al.* [12] and the association between T2D and AD is well-known. T2D appears to be a risk factor in both AD onset and a faster rate of progression, hypothesized to be due to common causal pathways between the two diseases [28, 29, 30]. While chronic pain does not emerge clearly in prior works clustering AD on EHRs, there does appear to be a relationship between chronic pain and AD/dementia [31, 32]. Any hypothetical causal link has yet to be established in this relationship, though it does appear that there is a bi-directional correlation. If chronic pain does indeed accelerate AD pathogenesis, then this would certainly warrant further investigation as a distinct phenotype of AD.

Cardiovascular or cerebrovascular disease clusters were found to some extent in all prior works clustering AD patient EHRs, and in combination with general diseases of aging and dermatological comorbidities, were enriched in clusters identified in this work, for both data modalities. For example, hypertension, hyperlipidemia, and dysrhythmias were reliably identified in one or both clustering analyses. With a number of common risk factors, there is a well-established link between cardiovascular disease and AD, as well as in other dementias [33, 34]. In addition to cardiovascular

disease, an increased prevalence of dermatological conditions were identified in this cluster in both analyses. It is unclear whether there is a general relationship between dermatological conditions and AD, though one review has explored the potential relationship [35]. Seborrheic keratosis was enriched for this cluster in the ICD clustering, and one study has linked its onset to overexpression of amyloid precursor protein, which plays an important role in AD pathogenesis [36]. For the ICD clustering, some chronic pain codes were also enriched in this cluster, though co-morbid with other diseases of aging, indicating some phenotypic overlap.

In the notes clustering, a cluster was found that was well-characterised by the prevalence of hydrocephalus as well as Lewy body disease (Lewy body dementia and Parkinson's). Hydrocephalus is a condition that results from a build-up of cerebrospinal fluid in the ventricles of the brain, and usually responds well to the placement of a shunt to drain excess fluid. While this cluster may not be representative of a distinct phenotype of AD, prior work has highlighted AD as a common source of comorbidity in patients with normal pressure hydrocephalus, and that AD status may limit the efficacy of shunt placement in patients presenting with both conditions [37, 38]. It has been suggested that the glymphatic (glia-lymphatic) system could be implicated in the relationship between AD and hydrocephalus [39]. The identification of this cluster may also represent a common diagnostic workflow, whereby the initial presentation for Lewy body disease may mimic that of hydrocephalus, with the conditions being common differential diagnoses for one another.

This study is limited by the lack of an independent validation cohort in which to validate the identified clusters. While this limitation is somewhat mitigated by the relative overlap in identified clusters between the ICD and notes representations, as well as the fact that many of the clusters identified here were also found in prior work, applying the same encoding and clustering technique on a hold-out validation cohort would strengthen the results presented here.

Furthermore, this study is limited by the lack of clear signal regarding which patients should belong to the AD phenotype, which is a by-product of the billing-motivated nature of coding, as well as the underlying diagnostic complexity associated with this disease and its related dementias. Instead of relying on the presence of an AD ICD code in a patient record to define the phenotype as done in previous work, which has its own limitations, we instead have used the cohort selection process to inform the definition of our target phenotype. While the majority of patients identified will be probable AD patients, this required expanding the focus of disease heterogeneity from just AD to related dementias as well.

Finally, this work could be improved by jointly leveraging the two data modalities utilised here, as well as expanding to more structured and unstructured data like medications and imaging. With a greater availability of multi-modal data, methodological improvements could be made by training a deep autoencoder to jointly leverage modalities, rather than performing two clustering analyses in parallel, and relying on the heuristic averaging employed here. In this framework, explicitly leveraging temporal or graph properties of EHRs may contribute to more informative representations and therefore improved unsupervised clustering, as prior approaches have demonstrated in a supervised learning setting [40, 41].

## References

- [1] Irma Mebane-Sims. 2009 alzheimer’s disease facts and figures. *Alzheimer’s & Dementia: The Journal of the Alzheimer’s Association*, 2009.
- [2] John Hardy and Dennis J Selkoe. The amyloid hypothesis of alzheimer’s disease: progress and problems on the road to therapeutics. *science*, 297(5580):353–356, 2002.
- [3] Ryan A Neff, Minghui Wang, Sezen Vatansever, Lei Guo, Chen Ming, Qian Wang, Erming Wang, Emrin Horgusluoglu-Moloch, Won-min Song, Aiqun Li, et al. Molecular subtyping of alzheimer’s disease using rna sequencing data reveals novel mechanisms and targets. *Science Advances*, 7(2):eabb5398, 2021.
- [4] Alexandra L Young, Razvan V Marinescu, Neil P Oxtoby, Martina Bocchetta, Keir Yong, Nicholas C Firth, David M Cash, David L Thomas, Katrina M Dick, Jorge Cardoso, et al. Uncovering the heterogeneity and temporal complexity of neurodegenerative diseases with subtype and stage inference. *Nature communications*, 9(1):1–16, 2018.
- [5] Jacob W Vogel, Alexandra L Young, Neil P Oxtoby, Ruben Smith, Rik Ossenkoppele, Olof T Strandberg, Renaud La Joie, Leon M Aksman, Michel J Grothe, Yasser Iturria-Medina, et al. Four distinct trajectories of tau deposition identified in alzheimer’s disease. *Nature Medicine*, 27(5):871–881, 2021.
- [6] David J Libon, Deborah AG Drabick, Tania Giovannetti, Catherine C Price, Mark W Bondi, Joel Eppig, Kathryn Devlin, Christine Nieves, Melissa Lamar, Lisa Delano-Wood, et al. Neuropsychological syndromes associated with alzheimer’s/vascular dementia: a latent class analysis. *Journal of Alzheimer’s disease*, 42(3):999–1014, 2014.
- [7] Nienke ME Scheltens, Francisca Galindo-Garre, Yolande AL Pijnenburg, Annelies E van der Vlies, Lieke L Smits, Teddy Koene, Charlotte E Teunissen, Frederik Barkhof, Mike P Wattjes, Philip Scheltens, et al. The identification of cognitive subtypes in alzheimer’s disease dementia using latent class analysis. *Journal of Neurology, Neurosurgery & Psychiatry*, 87(3):235–243, 2016.
- [8] Nienke ME Scheltens, Betty M Tijms, Teddy Koene, Frederik Barkhof, Charlotte E Teunissen, Steffen Wolfsgruber, Michael Wagner, Johannes Kornhuber, Oliver Peters, Brendan I Cohn-Sheehy, et al. Cognitive subtypes of probable alzheimer’s disease robustly identified in four cohorts. *Alzheimer’s & Dementia*, 13(11):1226–1236, 2017.
- [9] Finale Doshi-Velez, Yaorong Ge, and Isaac Kohane. Comorbidity clusters in autism spectrum disorders: an electronic health record time-series analysis. *Pediatrics*, 133(1):e54–e63, 2014.
- [10] Yuan Luo, Alal Eran, Nathan Palmer, Paul Avillach, Ami Levy-Moonshine, Peter Szolovits, and Isaac S Kohane. A multidimensional precision medicine approach identifies an autism subtype characterized by dyslipidemia. *Nature Medicine*, 26(9):1375–1379, 2020.
- [11] Xi Zhang, Jingyuan Chou, Jian Liang, Cao Xiao, Yize Zhao, Harini Sarva, Claire Henchcliffe, and Fei Wang. Data-driven subtyping of parkinson’s disease using longitudinal clinical records: a cohort study. *Scientific reports*, 9(1):1–12, 2019.
- [12] Jie Xu, Fei Wang, Zhenxing Xu, Prakash Adekkanattu, Pascal Brandt, Guoqian Jiang, Richard C Kiefer, Yuan Luo, Chengsheng Mao, Jennifer A Pacheco, et al. Data-driven discovery of probable alzheimer’s disease and related dementia subphenotypes using electronic health records. *Learning Health Systems*, 4(4):e10246, 2020.
- [13] Nonie Alexander, Daniel C Alexander, Frederik Barkhof, and Spiros Denaxas. Using unsupervised learning to identify clinical subtypes of alzheimer’s disease in electronic health records. *Studies in health technology and informatics*, 270:499–503, 2020.
- [14] Isotta Landi, Benjamin S Glicksberg, Hao-Chih Lee, Sarah Cherng, Giulia Landi, Matteo Danieletto, Joel T Dudley, Cesare Furlanello, and Riccardo Miotto. Deep representation learning of electronic health records to unlock patient stratification at scale. *NPJ digital medicine*, 3(1):1–11, 2020.
- [15] Zhe He, Shubo Tian, Arslan Erdengasileng, Neil Charness, and Jiang Bian. Temporal subtyping of alzheimer’s disease using medical conditions preceding alzheimer’s disease onset in electronic health records. *arXiv preprint arXiv:2202.10991*, 2022.
- [16] Alice S Tang, Tomiko Oskotsky, Shreyas Havaldar, William G Mantyh, Mesude Bicak, Caroline Warly Solsberg, Sarah Woldemariam, Billy Zeng, Zicheng Hu, Boris Oskotsky, et al. Deep phenotyping of alzheimer’s disease leveraging electronic medical records identifies sex-specific clinical associations. *Nature communications*, 13(1):1–15, 2022.
- [17] Ashish Vaswani, Noam Shazeer, Niki Parmar, Jakob Uszkoreit, Llion Jones, Aidan N Gomez, Łukasz Kaiser, and Illia Polosukhin. Attention is all you need. In *Advances in neural information processing systems*, pages 5998–6008, 2017.

- [18] Jacob Devlin, Ming-Wei Chang, Kenton Lee, and Kristina Toutanova. Bert: Pre-training of deep bidirectional transformers for language understanding. *arXiv preprint arXiv:1810.04805*, 2018.
- [19] Jinhyuk Lee, Wonjin Yoon, Sungdong Kim, Donghyeon Kim, Sunkyu Kim, Chan Ho So, and Jaewoo Kang. Biobert: a pre-trained biomedical language representation model for biomedical text mining. *Bioinformatics*, 36(4):1234–1240, 2020.
- [20] Emily Alsentzer, John R Murphy, Willie Boag, Wei-Hung Weng, Di Jin, Tristan Naumann, and Matthew McDermott. Publicly available clinical bert embeddings. *arXiv preprint arXiv:1904.03323*, 2019.
- [21] Alistair EW Johnson, Tom J Pollard, Lu Shen, H Lehman Li-Wei, Mengling Feng, Mohammad Ghassemi, Benjamin Moody, Peter Szolovits, Leo Anthony Celi, and Roger G Mark. Mimic-iii, a freely accessible critical care database. *Scientific data*, 3(1):1–9, 2016.
- [22] Youngduck Choi, Chill Yi-I Chiu, and David Sontag. Learning low-dimensional representations of medical concepts. *AMIA Summits on Translational Science Proceedings*, 2016:41, 2016.
- [23] Claude Elwood Shannon. A mathematical theory of communication. *The Bell system technical journal*, 27(3):379–423, 1948.
- [24] Nader Ebrahimi, Kurt Pflughoeft, and Ehsan S Soofi. Two measures of sample entropy. *Statistics & Probability Letters*, 20(3):225–234, 1994.
- [25] Pauli Virtanen, Ralf Gommers, Travis E. Oliphant, Matt Haberland, Tyler Reddy, David Cournapeau, Evgeni Burovski, Pearu Peterson, Warren Weckesser, Jonathan Bright, Stéfan J. van der Walt, Matthew Brett, Joshua Wilson, K. Jarrod Millman, Nikolay Mayorov, Andrew R. J. Nelson, Eric Jones, Robert Kern, Eric Larson, C J Carey, İlhan Polat, Yu Feng, Eric W. Moore, Jake VanderPlas, Denis Laxalde, Josef Perktold, Robert Cimrman, Ian Henriksen, E. A. Quintero, Charles R. Harris, Anne M. Archibald, Antônio H. Ribeiro, Fabian Pedregosa, Paul van Mulbregt, and SciPy 1.0 Contributors. SciPy 1.0: Fundamental Algorithms for Scientific Computing in Python. *Nature Methods*, 17:261–272, 2020.
- [26] F. Pedregosa, G. Varoquaux, A. Gramfort, V. Michel, B. Thirion, O. Grisel, M. Blondel, P. Prettenhofer, R. Weiss, V. Dubourg, J. Vanderplas, A. Passos, D. Cournapeau, M. Brucher, M. Perrot, and E. Duchesnay. Scikit-learn: Machine learning in Python. *Journal of Machine Learning Research*, 12:2825–2830, 2011.
- [27] Leland McInnes, John Healy, and James Melville. Umap: Uniform manifold approximation and projection for dimension reduction. *arXiv preprint arXiv:1802.03426*, 2018.
- [28] Zoe Arvanitakis, Robert S Wilson, Julia L Bienias, Denis A Evans, and David A Bennett. Diabetes mellitus and risk of alzheimer disease and decline in cognitive function. *Archives of neurology*, 61(5):661–666, 2004.
- [29] Ramit Ravona-Springer, Xiaodong Luo, James Schmeidler, Michael Wysocki, Gerson Lesser, Michael Rapp, Karen Dahlman, Hillel Grossman, Vahram Haroutunian, and Michal Schnaider Beeri. Diabetes is associated with increased rate of cognitive decline in questionably demented elderly. *Dementia and geriatric cognitive disorders*, 29(1):68–74, 2010.
- [30] Catrina Sims-Robinson, Bhumsoo Kim, Andrew Rosko, and Eva L Feldman. How does diabetes accelerate alzheimer disease pathology? *Nature Reviews Neurology*, 6(10):551–559, 2010.
- [31] Elizabeth L Whitlock, L Grisell Diaz-Ramirez, M Maria Glymour, W John Boscardin, Kenneth E Covinsky, and Alexander K Smith. Association between persistent pain and memory decline and dementia in a longitudinal cohort of elders. *JAMA internal medicine*, 177(8):1146–1153, 2017.
- [32] Song Cao, Daniel W Fisher, Tain Yu, and Hongxin Dong. The link between chronic pain and alzheimer’s disease. *Journal of neuroinflammation*, 16(1):1–11, 2019.
- [33] IJ Martins, Eugene Hone, JK Foster, SI Sünram-Lea, Anastazija Gnjec, SJ Fuller, D Nolan, SE Gandy, and RN Martins. Apolipoprotein e, cholesterol metabolism, diabetes, and the convergence of risk factors for alzheimer’s disease and cardiovascular disease. *Molecular psychiatry*, 11(8):721–736, 2006.
- [34] Heather M Snyder, Roderick A Corriveau, Suzanne Craft, James E Faber, Steven M Greenberg, David Knopman, Bruce T Lamb, Thomas J Montine, Maiken Nedergaard, Chris B Schaffer, et al. Vascular contributions to cognitive impairment and dementia including alzheimer’s disease. *Alzheimer’s & Dementia*, 11(6):710–717, 2015.
- [35] Hanlin Zhang, Dingyue Zhang, Keyun Tang, and Qiuning Sun. The relationship between alzheimer’s disease and skin diseases: A review. *Clinical, cosmetic and investigational dermatology*, 14:1551, 2021.
- [36] Yuanying Li, Yu Wang, Wei Zhang, Leiwei Jiang, Wenming Zhou, Zhi Liu, Shijun Li, and Hongguang Lu. Overexpression of amyloid precursor protein promotes the onset of seborrheic keratosis and is related to skin ageing. *Acta Dermato-Venereologica*, 98(6), 2018.

- [37] Roy Hamilton, Sunil Patel, Edward B Lee, Eric M Jackson, Joanna Lopinto, Steven E Arnold, Christopher M Clark, Anuj Basil, Leslie M Shaw, Sharon X Xie, et al. Lack of shunt response in suspected idiopathic normal pressure hydrocephalus with alzheimer disease pathology. *Annals of neurology*, 68(4):535–540, 2010.
- [38] Danielle Cabral, Thomas G Beach, Linda Vedders, Lucia I Sue, Sandra Jacobson, Kent Myers, and Marwan N Sabbagh. Frequency of alzheimer’s disease pathology at autopsy in patients with clinical normal pressure hydrocephalus. *Alzheimer’s & Dementia*, 7(5):509–513, 2011.
- [39] Benjamin C Reeves, Jason K Karimy, Adam J Kundishora, Humberto Mestre, H Mert Cerci, Charles Matouk, Seth L Alper, Iben Lundgaard, Maiken Nedergaard, and Kristopher T Kahle. Glymphatic system impairment in alzheimer’s disease and idiopathic normal pressure hydrocephalus. *Trends in molecular medicine*, 26(3):285–295, 2020.
- [40] Weicheng Zhu and Narges Razavian. Variationally regularized graph-based representation learning for electronic health records. In *Proceedings of the Conference on Health, Inference, and Learning*, pages 1–13, 2021.
- [41] Edward Choi, Zhen Xu, Yujia Li, Michael Dusenberry, Gerardo Flores, Emily Xue, and Andrew Dai. Learning the graphical structure of electronic health records with graph convolutional transformer. In *Proceedings of the AAAI Conference on Artificial Intelligence*, volume 34, pages 606–613, 2020.

## Supplementary Material

### Enriched ICD9 codes in ICD Clusters

The following tables show the top-20 ICD codes for each of the clusters identified in both the ICD and patient notes clustering analyses. They also provide information on the significance and relative prevalence of each of the codes within and between clusters.

**Key:**

- **ICD Code:** ICD9 code
- **p\_value:**  $p$ -value from  $\chi^2$  test.
- **p\_value\_fdr:** Bonferroni-corrected  $p$ -value.
- **Sig.:** Statistical significance following correction for multiple comparisons, \*\* < 0.001; \* < 0.01; \* < 0.05.
- **Prev.:** Prevalence of code within cluster.
- **Exp. Prev.:** Expected prevalence, prevalence of code in other clusters.
- **fc:** Fold-change between observed prevalence and expected prevalence.
- **DiagnosisNM:** ICD9 code name.

ICD Code	p_value	p_value_fdr	Sig.	Prev.	Exp. Prev.	fc	DiagnosisNM
338.29	4.80E-122	2.74E-118	***	0.62598	0.17930	3.491	Other chronic pain
724.2	8.10E-116	4.63E-112	***	0.54724	0.14391	3.803	Bilateral low back pain without sciatica
729.5	8.45E-110	4.83E-106	***	0.61417	0.18668	3.290	Foot pain
729.1	2.99E-98	1.71E-94	***	0.30118	0.05099	5.907	Fibromyalgia
721.3	1.45E-97	8.31E-94	***	0.28346	0.04529	6.259	Spondylosis of lumbar region without myelopathy or radiculopathy
786.2	6.60E-97	3.77E-93	***	0.55118	0.16639	3.313	Cough
724.4	1.60E-96	9.15E-93	***	0.29331	0.04914	5.968	Thoracic or lumbosacral neuritis or radiculitis, unspecified
780.79	1.86E-94	1.07E-90	***	0.59055	0.19239	3.070	Malaise and fatigue
357.2	2.93E-93	1.68E-89	***	0.21063	0.02499	8.428	Type 2 diabetes mellitus with diabetic polyneuropathy
719.45	3.31E-90	1.89E-86	***	0.38583	0.08990	4.292	Pain in joint, pelvic region and thigh
V58.67	3.91E-89	2.24E-85	***	0.21457	0.02751	7.800	Diabetes mellitus type 2, insulin dependent
V58.69	4.12E-87	2.36E-83	***	0.32480	0.06642	4.890	Encounter for long-term (current) use of other medications
530.81	3.20E-84	1.83E-80	***	0.44291	0.12278	3.607	Gastroesophageal reflux disease without esophagitis
786.05	1.70E-80	9.69E-77	***	0.32480	0.07112	4.567	SOB (shortness of breath)
V58.89	2.04E-79	1.16E-75	***	0.43504	0.12395	3.510	Excoriation of back, unspecified laterality, subsequent encounter
250.60	2.99E-79	1.71E-75	***	0.21063	0.03019	6.977	Type 2 diabetes mellitus with autonomic neuropathy
780.96	1.70E-78	9.69E-75	***	0.38583	0.10030	3.847	Pain
296.32	5.01E-77	2.87E-73	***	0.20866	0.03053	6.835	Major depressive disorder, recurrent episode, moderate
V65.49	1.24E-75	7.09E-72	***	0.48425	0.15548	3.114	Other specified counseling
786.50	1.89E-74	1.08E-70	***	0.36220	0.09292	3.898	Chest pain, unspecified chest pain type

Table S1: Top 20 enriched codes for chronic pain/T2D cluster in the ICD clustering.

ICD Code	p_value	p_value_fdr	Sig.	Prev.	Exp. Prev.	fc	DiagnosisNM
331.0	1.30E-21	7.42E-18	***	0.50046	0.37406	1.338	Alzheimer's dementia
294.10	1.86E-12	1.06E-08	***	0.48621	0.39292	1.237	Alzheimer's dementia
331.19	1.90E-10	1.09E-06	***	0.07678	0.03538	2.170	Frontotemporal dementia
294.11	8.34E-08	0.000476948	***	0.25540	0.19481	1.311	Dementia due to medical condition with behavioral disturbance
V65.9	6.45E-07	0.003687954	**	0.08943	0.05377	1.663	Encounter for consultation
335.20	0.006012318	34.37843242		0.01080	0.00377	2.863	Motor neuron disease
331.6	0.011095009	63.44126254		0.00943	0.00330	2.855	Corticobasal degeneration
784.3	0.020494271	117.1862438		0.07494	0.05896	1.271	Primary progressive aphasia
333.0	0.141054986	806.5524072		0.01747	0.01226	1.425	Neurogenic orthostatic hypotension
784.69	0.174142823	995.7486616		0.01977	0.01462	1.352	Apraxia
293.84	0.198053555	1132.470228		0.02322	0.01792	1.295	Anxiety disorder due to medical condition
290.20	0.206186693	1178.975511		0.00483	0.00236	2.047	Dementia, senile with delusions
345.91	0.230943349	1320.534071		0.00207	0.00047	4.386	Intractable epilepsy without status epilepticus
331.11	0.247924607	1417.632902		0.01310	0.00943	1.389	Pick's disease
334.2	0.277332277	1585.785958		0.00851	0.00566	1.503	Corticobasal syndrome
331.9	0.286177934	1636.365427		0.02851	0.02358	1.209	Cerebral degeneration, unspecified
046.19	0.352705118	2016.767865		0.00299	0.00142	2.112	Dementia associated with Jakob-Creutzfeldt disease
742.3	0.39801109	2275.827412		0.00161	0.00047	3.411	Congenital hydrocephalus
319	0.477699593	2731.486275		0.00207	0.00094	2.193	Mental retardation
783.4	0.522523203	2987.787672		0.00138	0.00047	2.924	Development delay

Table S2: Top 20 enriched codes for other neuro cluster in ICD clustering.

ICD Code	p_value	p_value_fdr	Sig.	Prev.	Exp. Prev.	fc	DiagnosisNM
V70.0	6.52E-189	3.73E-185	***	0.71774	0.30342	2.366	Routine general medical examination at a health care facility
401.9	2.44E-138	1.39E-134	***	0.70906	0.35138	2.018	Essential hypertension
702.0	3.06E-130	1.75E-126	***	0.33685	0.08748	3.850	AK (actinic keratosis)
702.19	1.56E-126	8.91E-123	***	0.39826	0.12598	3.161	Seborrheic keratoses
338.29	1.44E-124	8.23E-121	***	0.42494	0.14450	2.941	Other chronic pain
729.5	9.46E-120	5.41E-116	***	0.42866	0.15109	2.837	Foot pain
272.4	1.79E-111	1.03E-107	***	0.52481	0.22828	2.299	Other and unspecified hyperlipidemia
786.2	2.20E-99	1.26E-95	***	0.37841	0.13627	2.777	Cough
238.2	5.25E-93	3.00E-89	***	0.25993	0.07019	3.703	Neoplasm of uncertain behavior of skin
780.79	1.18E-92	6.75E-89	***	0.40757	0.16262	2.506	Malaise and fatigue
V10.83	7.82E-85	4.47E-81	***	0.23697	0.06340	3.738	History of basal cell cancer
709.09	3.66E-84	2.10E-80	***	0.27295	0.08399	3.250	Other dyschromia
216.9	3.89E-83	2.22E-79	***	0.24504	0.06896	3.553	Nevus
V03.89	1.89E-80	1.08E-76	***	0.80397	0.53643	1.499	Encounter for immunization
719.46	1.05E-75	6.03E-72	***	0.29467	0.10436	2.823	Pain, joint, knee
724.2	2.37E-74	1.36E-70	***	0.32568	0.12577	2.589	Bilateral low back pain without sciatica
272.0	1.07E-73	6.11E-70	***	0.37965	0.16385	2.317	Pure hypercholesterolemia
V72.84	1.92E-73	1.10E-69	***	0.30769	0.11486	2.679	Pre-operative examination
V58.89	5.43E-71	3.10E-67	***	0.28536	0.10292	2.773	Excoriation of back, unspecified laterality, subsequent encounter
788.41	9.11E-70	5.21E-66	***	0.25558	0.08563	2.985	Urinary frequency

Table S3: Top 20 enriched codes for cardiovascular/aging cluster in ICD clustering.

Enriched ICD9 codes in Notes Clusters

ICD Code	p_value	p_value_fdr	Sig.	Prev.	Exp. Prev.	fc	DiagnosisNM
331.5	8.44E-60	4.36E-56	***	0.12594	0.02340	5.383	Idiopathic normal pressure hydrocephalus (INPH)
V45.2	9.08E-30	4.69E-26	***	0.04629	0.00540	8.574	Ventriculopleural shunt status
331.4	5.83E-27	3.01E-23	***	0.05786	0.01100	5.261	Hydrocephalus
332.0	1.26E-21	6.50E-18	***	0.13342	0.05819	2.293	Parkinson disease
331.82	3.03E-21	1.56E-17	***	0.10551	0.04079	2.587	Dementia with Lewy bodies
348.89	5.34E-20	2.76E-16	***	0.05718	0.01480	3.864	Other conditions of brain(348.89)
781.2	7.18E-14	3.71E-10	***	0.27093	0.18136	1.494	Abnormality of gait and mobility
331.3	2.10E-10	1.08E-06	***	0.02519	0.00580	4.343	Communicating hydrocephalus
V65.9	4.72E-06	0.024394252	*	0.10619	0.06939	1.530	Encounter for consultation
781.3	0.000315501	1.629247132		0.04969	0.02979	1.668	Ataxia
046.19	0.000455391	2.351639622		0.00681	0.00120	5.674	Dementia associated with Jakob-Creutzfeldt disease
356.9	0.000559522	2.889370481		0.06263	0.04079	1.535	Unspecified hereditary and idiopathic peripheral neuropathy
458.0	0.001249156	6.450643386		0.04221	0.02559	1.649	Orthostatic hypotension
780.39	0.001310365	6.766726181		0.08237	0.05859	1.406	Seizures, generalized convulsive
136.9	0.001746166	9.01719964		0.00817	0.00220	3.714	Infection
E942.2	0.002219494	11.46146762		0.00340	0.00020	17.022	Statin-induced myositis
279.3	0.002219494	11.46146762		0.00340	0.00020	17.022	Immune deficiency disorder
781.1	0.003508	18.11531209		0.02110	0.01080	1.954	Anosmia
V42.0	0.003635117	18.77174336		0.00613	0.00140	4.377	Kidney replaced by transplant
294.11	0.003721492	19.21778421		0.26413	0.22715	1.163	Dementia due to medical condition with behavioral disturbance

Table S4: Top 20 enriched codes for hydrocephalus/LBD cluster in notes clustering.

ICD Code	p_value	p_value_fdr	Sig.	Prev.	Exp. Prev.	fc	DiagnosisNM
290.0	2.29E-100	1.18E-96	***	0.23978	0.05123	4.681	Senile dementia
401.1	2.62E-06	0.013535797	*	0.17656	0.12604	1.401	Essential hypertension, benign
331.0	3.78E-05	0.195187341		0.51041	0.44616	1.144	Alzheimer's dementia
692.74	4.95E-05	0.255842387		0.04318	0.02242	1.925	Diffuse photoaging of skin
348.30	0.000137693	0.711045922		0.03701	0.01894	1.954	Encephalopathy, unspecified
709.9	0.000431726	2.22943438		0.10100	0.07133	1.416	Disorder of skin and subcutaneous tissue
427.89	0.000502806	2.59649085		0.09792	0.06901	1.419	Other specified cardiac dysrhythmias(427.89)
562.12	0.000575282	2.970755233		0.00463	0.00039	11.965	Diverticulosis of large intestine with hemorrhage
414.00	0.000607857	3.138971122		0.12953	0.09666	1.340	Mild coronary artery disease
921.1	0.000936006	4.833534464		0.00694	0.00135	5.128	Periorbital ecchymosis of right eye
V53.2	0.001189183	6.140943366		0.02699	0.01373	1.966	Encounter for fitting or adjustment of hearing aid
443.81	0.001993231	10.29304402		0.02082	0.00986	2.112	Type II diabetes mellitus with peripheral circulatory disorder
780.93	0.002661917	13.74613804		0.50810	0.46105	1.102	Memory loss
512.89	0.003442329	17.77618542		0.00386	0.00039	9.971	Spontaneous pneumothorax
366.52	0.00366121	18.90648649		0.00848	0.00251	3.375	Posterior capsular opacification of right eye, not obscuring vision
173.32	0.005218198	26.94677658		0.02082	0.01063	1.958	Squamous cell carcinoma of skin of other and unspecified parts of face
173.81	0.005252131	27.12200313		0.00308	0.00019	15.954	Basal cell carcinoma of overlapping sites of skin
292.81	0.005252131	27.12200313		0.00308	0.00019	15.954	Confusion caused by a drug
581.9	0.005252131	27.12200313		0.00308	0.00019	15.954	Nephrosis
V54.15	0.007277841	37.58277194		0.00617	0.00155	3.988	Closed fracture of femoral condyle, right, with routine healing, subsequent encounter

Table S5: Top 20 enriched codes for cardiovascular/aging cluster in notes clustering.

ICD Code	p_value	p_value_fdr	Sig.	Prev.	Exp. Prev.	fc	DiagnosisNM
799.59	2.97E-20	1.53E-16	***	0.17846	0.09689	1.842	Cognitive complaints with normal exam
293.83	1.36E-19	7.02E-16	***	0.05562	0.01229	4.524	Mood disorder in conditions classified elsewhere
293.84	2.27E-19	1.17E-15	***	0.03564	0.00253	14.082	Anxiety disorder due to medical condition
294.9	3.88E-18	2.00E-14	***	0.32046	0.22234	1.441	Unspecified persistent mental disorders due to conditions classified elsewhere
784.3	3.81E-17	1.97E-13	***	0.09287	0.03868	2.401	Primary progressive aphasia
V79.0	3.65E-15	1.89E-11	***	0.07208	0.02748	2.623	Screening for depression
294.8	1.42E-11	7.33E-08	***	0.10367	0.05640	1.838	Other persistent mental disorders due to conditions classified elsewhere
331.19	6.06E-11	3.13E-07	***	0.08045	0.04013	2.005	Frontotemporal dementia
799.52	8.60E-10	4.44E-06	***	0.05130	0.02133	2.405	Cognitive communication deficit
290.40	6.89E-09	3.56E-05	***	0.11663	0.07303	1.597	Vascular dementia without behavioral disturbance
V76.10	2.26E-08	0.000116505	***	0.13661	0.09111	1.499	Breast screening
V77.91	2.54E-07	0.001311741	**	0.06263	0.03398	1.843	Screening for lipid disorders
312.9	1.21E-06	0.00623477	**	0.05022	0.02603	1.929	Cognitive and behavioral changes
780.96	1.43E-06	0.007383663	**	0.13985	0.09978	1.402	Pain
327.01	1.69E-06	0.0087282	**	0.02781	0.01048	2.652	Insomnia due to medical condition classified elsewhere
V76.51	1.89E-06	0.009737959	**	0.09125	0.05893	1.548	Special screening for malignant neoplasms, colon
327.23	2.76E-06	0.014258581	*	0.14363	0.10412	1.379	Obstructive sleep apnea (adult) (pediatric)
V82.81	2.96E-06	0.015304732	*	0.05346	0.02928	1.825	Screening for osteoporosis
799.55	1.19E-05	0.061544119		0.03429	0.01627	2.108	Frontal lobe and executive function deficit
V03.82	1.22E-05	0.062936385		0.05724	0.03362	1.702	Need for Streptococcus pneumoniae vaccination

Table S6: Top 20 enriched codes for other neuro cluster in notes clustering.

## Cluster Comparison

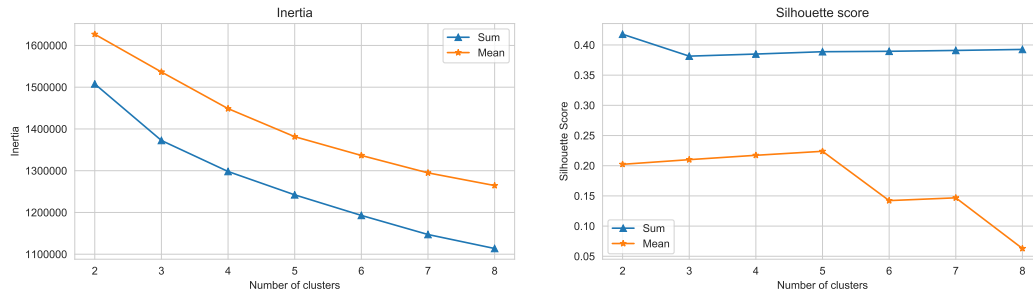


Figure S1: Inertia (within-cluster sum of squares, left) and silhouette score (right) and as a function of number of clusters and embedding methodology for the ICD clustering.

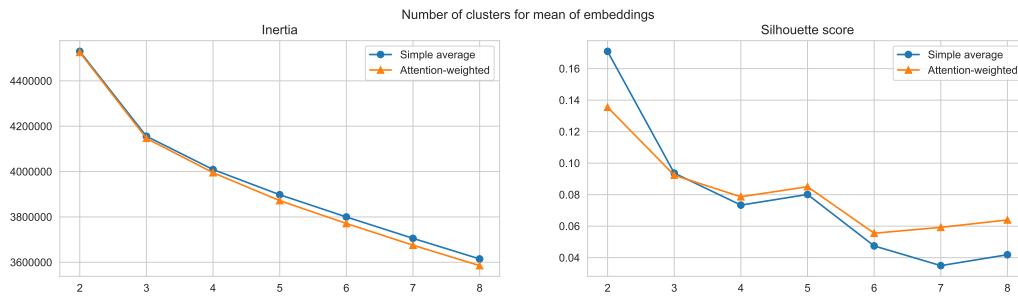


Figure S2: Inertia (within-cluster sum of squares, left) and silhouette score (right) as a function of number of clusters and embedding methodology for the patient notes clustering.

## Attention Heatmaps

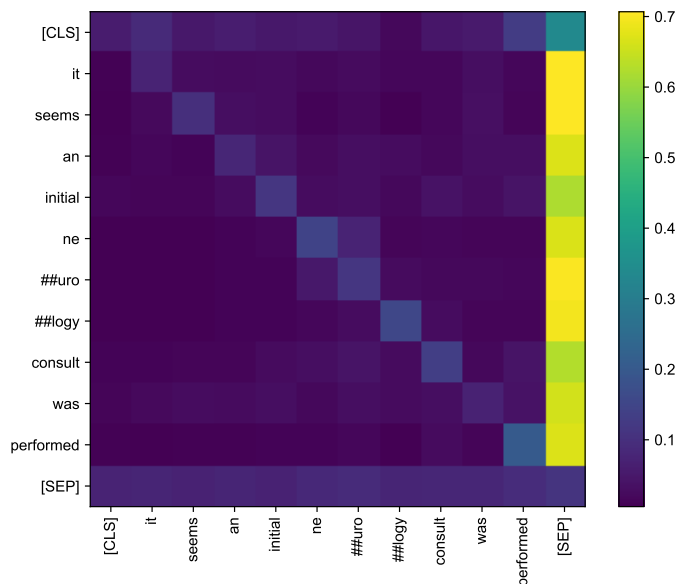


Figure S3: Attention heatmap of final layer for example input sequence, averaged over all 12 attention heads. This attention matrix exhibits high attention weights to the [SEP] token for most tokens, and slightly higher row-wise entropy (and therefore higher weight in averaging) for ‘initial’ and ‘consult’.

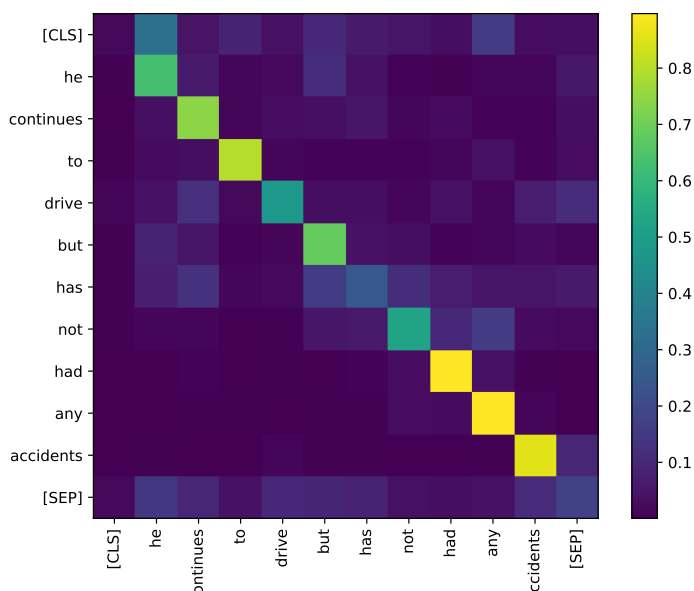


Figure S4: Attention heatmap of final layer for example input sequence, for head 3 alone. Most tokens attend heavily to themselves, indicating relatively low row-wise entropy. Examples of tokens with higher-row wise entropy that attend to multiple tokens include ‘drive’, ‘has’, and ‘not’.